

# Wide-field coherent anti-Stokes Raman scattering microscopy with non-phase-matching illumination

I. Toytman,<sup>1</sup> K. Cohn,<sup>1</sup> T. Smith,<sup>1</sup> D. Simanovskii,<sup>1,\*</sup> and D. Palanker<sup>1,2</sup>

<sup>1</sup>Hansen Experimental Physics Laboratory, Stanford University, 445 Via Palou, Stanford, California 94305, USA

<sup>2</sup>Department of Ophthalmology, Stanford University School of Medicine, 300 Pasteur Drive, Stanford, California 94305, USA

\*Corresponding author: simanovskii@stanford.edu

Received February 13, 2007; revised May 1, 2007; accepted May 9, 2007;  
posted May 10, 2007 (Doc. ID 80079); published June 26, 2007

We have developed and tested a wide-field coherent anti-Stokes Raman scattering (CARS) microscopy technique, which provides the simultaneous imaging of an extended illuminated area without scanning. This method is based on the non-phase-matching illumination of a sample and imaging of a CARS signal with a CCD camera using conventional microscope optics. We have identified a set of conditions on the illumination and imaging optics, as well as on sample preparation. Imaging of test objects proved high spatial resolution and chemical selectivity of this technique. © 2007 Optical Society of America

OCIS codes: 180.0180, 190.5650, 190.5890.

In recent years, significant interest in new optical techniques allowing for the imaging of living cells with intrinsic chemical contrast has been evident. One of the methods, which has attracted particular attention, is coherent anti-Stokes Raman scattering (CARS) microscopy [1]. Similar to spontaneous Raman scattering, CARS is greatly enhanced in the vicinity of molecular vibrational resonances. The coherent nature of this process can make a CARS signal much greater than that of spontaneous Raman scattering [2]. However, for coherent signal enhancement, constructive interference must be established over some interaction length, which imposes certain limitations on axial resolution attainable in CARS microscopy.

Most of the CARS microscopes developed so far are based on the scanning of tightly focused copropagating beams [3,4]. Objectives with large numerical apertures produce focal spots with diameters and lengths of the order of a micrometer, or even less. Small interaction length usually results in CARS signals of low intensity, however inherently constant interaction length allows for straightforward image interpretation. Only recently, scanning CARS microscopes operating at a video rate (30 Hz) have been demonstrated [5]. These microscopes utilize lasers and parametric oscillators operating at a very high (~80 MHz) repetition rate, which allows for a manifold signal averaging over each frame. Such averaging is essential to compensate for low signal levels and for laser instabilities.

In this Letter we explore a wide-field illumination scheme for CARS microscopy, in which the whole image is registered simultaneously—similar to conventional microscopy with a focal plane array detector. Such microscopes could have faster image acquisition rates and significantly relaxed requirements on laser stability. The first known attempt at building a wide-field CARS microscope was undertaken by Heinrich *et al.* [6,7] The phase-matching illumination geom-

etry implemented in that design resulted in the generation of a strong background CARS signal from the bulk medium, which, in our opinion, limited the chemical selectivity of the method.

To prevent CARS generation in a homogeneous bulk material, we used a non-phase-matching sample illumination and relied on light refraction or scattering within the sample, which brings some portion of the incident radiation into the phase-matching condition. Thus, a CARS signal is generated only in the presence of a scattering or refracting object. If such an object, or its immediate surrounding, contains molecules with Raman-active vibrational modes, the CARS signal will be greatly enhanced. In this respect, such illumination geometry resembles dark-field illumination in conventional microscopy. However, nonlinear optical transformation gives to this technique a new quality—the CARS signal—which depends on the optical properties of the object and its chemical composition. Spatial resolution of this technique is determined by the diffraction limit of the imaging objective, provided that CARS radiation fills its aperture completely. For the broad illumination angles used in our setup, this condition is generally fulfilled.

This approach is potentially applicable to thick samples. Images of a sample at each particular depth are obtained by bringing the sample to the focal plane of the imaging optics. However, in the case of optically thick samples, i.e., when radiation undergoes multiple scattering, the CARS signal generated on one object will illuminate other objects, thus reducing the chemical contrast of the image. In addition, scattered pump and Stokes beams may fall under the phase-matching condition in the bulk-producing background CARS signal.

We tested the proposed technique using an experimental setup built around an inverted microscope (Axiovert 35, Carl Zeiss, Germany). We used 800 nm radiation generated by a Ti:sapphire regenerative

amplifier as the pump beam, and the frequency doubled signal from an optical parametric amplifier (Spectra-Physics, Calif), tunable in the range of 1017–1055 nm, was used as the Stokes beam. Sample illumination geometry is shown schematically in Fig. 1. Both beams were focused onto the sample to a spot of about 200  $\mu\text{m}$  in diameter. The pump laser was focused with a 500 mm focal length lens, which practically produced a parallel beam on the sample. The Stokes beam was focused through a  $100\times 0.73$  NA microscope objective, which created a broad range of incidence angles. To control the angular range of the Stokes beam, a circular mask was placed at the objective's output, blocking the central part of the beam and eliminating the component collinear with the pump beam. The CARS signal was detected through the same microscope objective.

Initially the pump and the Stokes beams were nearly counterpropagating in the sample, which prevented CARS generation both in the sample and bulk. After reflection from the dichroic mirror transparent at the pump wavelength, the Stokes beam became almost copropagating with the pump, and even small angle scattering brought pump and Stokes beams into the phase-matching condition.

By placing the sample directly onto the mirror surface we minimized the distance that laser beams nearly copropagate within bulk material before hitting the sample. In this geometry, backlight illumination of the sample by the background CARS signal

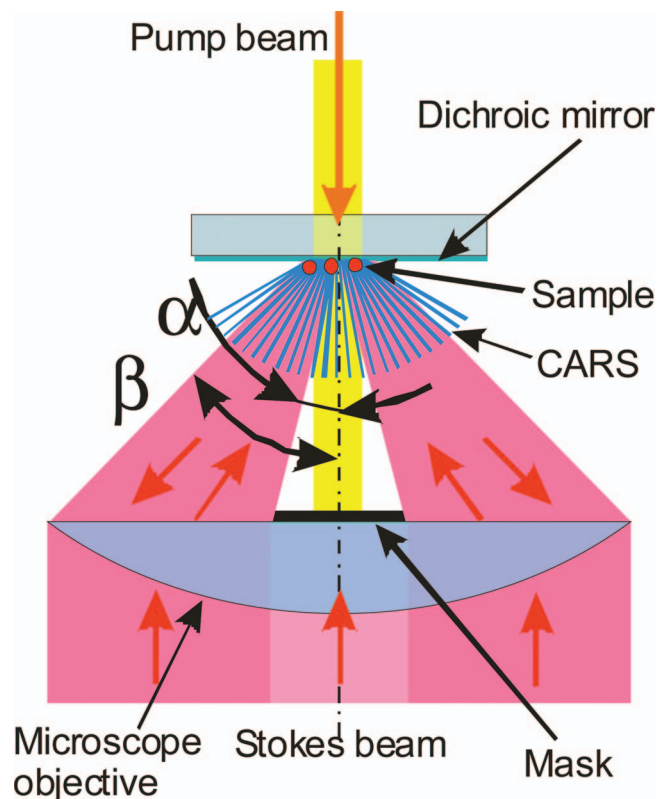


Fig. 1. Wide-field illumination geometry. The pump beam goes through the sample positioned on a dichroic mirror. The Stokes is focused by a microscope objective and is reflected from the mirror. The central part of the Stokes beam is blocked by a circular mask. The CARS signal is collected by the same objective.

was negligible. However, some CARS generation in the bulk below the sample (water layer, thin Mylar film, or glass coverslip) is still possible. To minimize its level, the angular spread of the Stokes beam  $\beta$ – $\alpha$  was precisely controlled and optimized for the particular sample configurations.

Our amplified laser system generated pump pulses with energy up to 200  $\mu\text{J}$  and Stokes pulses up to 10  $\mu\text{J}$ . Both pulses were about 1 ps long, had  $10$ – $20\text{ cm}^{-1}$  spectral width and provided fluence close to the damage threshold in a spot of  $\sim 200\text{ }\mu\text{m}$ . To achieve a relatively homogeneous illumination we used the central part (100  $\mu\text{m}$ ) of the focal spots of the pump and Stokes beams, which provided a moderate ( $\sim 30\%$ ) variation in the intensity from the center to the edges of the field of view. To decrease speckling, which is inherent to the wide-field imaging with coherent light, the Stokes beam was delivered through a 1 m long multimode (500  $\mu\text{m}$  thick) optical fiber, which was randomly waggled. Averaging over 100 shots reduced speckling-related intensity modulation in the CARS image to the level of a few percent.

CARS images formed by a microscope objective were acquired by a 2D liquid nitrogen cooled CCD array (CCD-512-TKB/1/VISAR, Princeton Instruments, New Jersey). The size of the imaged area was  $100\times 100\text{ }\mu\text{m}$ . For a number of measurements that did not require spatial resolution, the CARS signal was collected by a photomultiplier (PMT, Hamamatsu, Japan). This proved to be very convenient for the rapid optimization of the delay between the pump and Stokes beams, and also for the measurements of the spectral, intensity, and angular dependencies of the CARS signal. In both cases a set of notch filters was used to filter out residual pump and Stokes radiation. It had 75% transmission at the CARS wavelength and less than  $10^{-6}$  at the pump and Stokes.

It was found that the detected signal depends quadratically on the pump and linearly on the Stokes beam intensities up to the pump fluence of  $100\text{ mJ/cm}^2$ , and no signal was detected when the pump and Stokes beams were not overlapping in time. This type of behavior is a clear signature of CARS interaction with no contribution from multiphoton luminescence and some other effects. To evaluate the effectiveness of the background CARS signal suppression in the bulk environment, we compared the angular dependence of the CARS signal generated in a thick transparent sample (100  $\mu\text{m}$  thick glass coverslip) to that generated in small scattering objects (6  $\mu\text{m}$  polystyrene beads deposited directly onto the dichroic mirror). The CARS signal generated in both samples is plotted in Fig. 2 as a function of the minimal illumination angle of the Stokes beam,  $\alpha$ . As expected, at  $\alpha=0^\circ$ , a strong CARS signal was generated in the glass coverslip because of phase matching between the pump and the collinear component of the Stokes beam. However, with increasing  $\alpha$ , the CARS signal rapidly decreased, and at  $\alpha=10^\circ$  it was reduced by 2 orders of magnitude. At the same time, CARS generated by the polystyrene

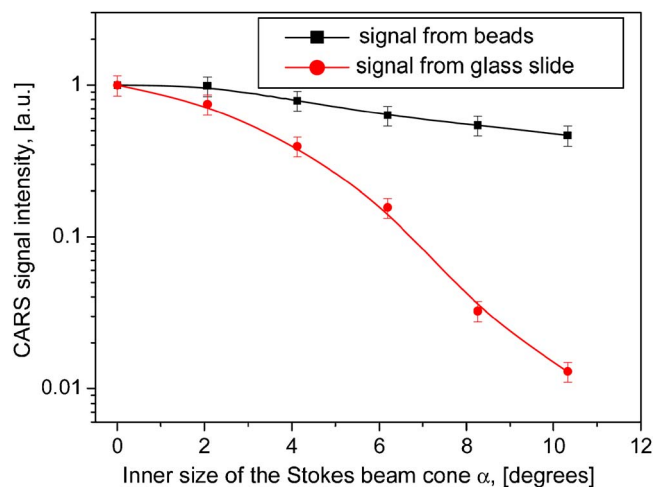


Fig. 2. (Color online) Normalized dependencies of the CARS signals from a polystyrene bead (small scattering object) and a glass coverslip (extended homogeneous material) as a function of the blocked angle of the Stokes beam,  $\alpha$ .

beads exhibited much weaker angular dependence, which in the first approximation could be attributed to the reduced aperture of the collecting objective. In this way, phase matching—and thus CARS generation—in a nonscattering bulk sample can be effectively suppressed by blocking the central portion of the angled Stokes beam. For all further measurements angle  $\alpha$  was set to  $10^\circ$ .

In order to demonstrate the chemical selectivity and spatial resolution of our wide-field CARS technique, we compared images of objects of the same shape, but different chemical composition, namely, polystyrene and quartz beads, both  $6\ \mu\text{m}$  in diameter. CARS spectra have been acquired from polystyrene and quartz beads by scanning the Raman shift from  $2700$  to  $3150^\circ$ . At the aromatic resonance ( $3071\ \text{cm}^{-1}$ ), polystyrene beads generate a signal more than five times stronger signal than that of the off resonance ( $3116\ \text{cm}^{-1}$ ). The glass beads, however, exhibited practically no spectral dependence within this range.

Images of a mixture of polystyrene and quartz beads floating in a thin ( $\sim 30\ \mu\text{m}$ ) layer of water between the dichroic mirror and a  $3\ \mu\text{m}$  Mylar film were taken on and off aromatic resonance and are shown in Figs. 3(a) and 3(b), respectively. Acquisition time as well as pump and Stokes intensities were kept constant in both cases. As expected, the brightness of the quartz beads was practically the same in both cases, whereas the brightness of the polystyrene beads was considerably higher on resonance. It is interesting to note that, even out of the resonance, polystyrene beads appeared significantly brighter than quartz ones. This could be attributed to different nonlinear constants of these materials and also to the higher refractive index of polystyrene beads ( $n_{\text{polystyrene}}=1.59$  versus  $n_{\text{quartz}}=1.46$ ). A higher index leads to a stronger refraction of the laser beams in the polystyrene beads, which is a key condition for

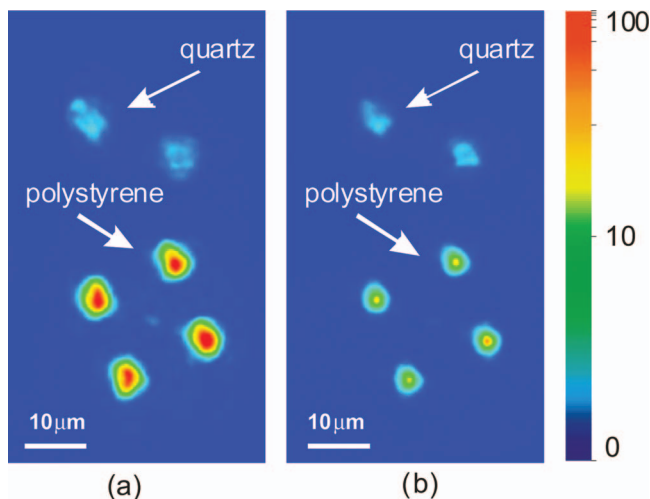


Fig. 3. Images of the glass and polystyrene beads taken at (a) the  $3071\ \text{cm}^{-1}$  resonance and (b) out of resonance at  $3116\ \text{cm}^{-1}$  (b).

CARS generation in the non-phase-matching illumination geometry.

In conclusion, we have developed a method for a non-scanning wide-field CARS imaging, that allows for fast image acquisition, high spatial resolution, and chemical selectivity. As opposed to scanning CARS microscopy, where spatial resolution is set by illumination optics, in a wide-field technique, it is determined by the imaging optics, similar to conventional microscopy. We have shown that a precisely controlled non-phase-matching illumination geometry, similar to dark-field illumination, is critical for the suppression of the bulk signal and thus for the reliable imaging of small objects in transparent media. The viability of the method was confirmed by the analysis of the CARS signals and with images of well-defined test objects. We expect that the fine tuning of the illumination conditions will allow for high quality wide-field CARS imaging of living cells and tissues.

This work was supported by the U.S. Air Force Office of Scientific Research (AFOSR) (contract FA9550-04-01-0075).

## References

1. A. Volkmer, *J. Phys. D* **38**, R59 (2005).
2. B. S. Hudson, *New Laser Techniques for Biophysical Studies*, L. J. Mullins, ed., Vol. 6 of *Annual Review of Biophysics and Bioengineering* (Annual Reviews, 1977), 135–150.
3. M. D. Duncan, J. Reintjes, and T. J. Manuccia, *Opt. Lett.* **7**, 350 (1982).
4. C. Ji-Xin, Y. K. Jia, Z. Gengfeng, and X. S. Xie, *Biophys. J.* **83**, 502 (2002).
5. C. L. Evans, E. O. Potma, M. Puoris'haag, D. Cote, C. P. Lin, and X. S. Xie, *Proc. Natl. Acad. Sci. U.S.A.* **102**, 16807 (2005).
6. C. Heinrich, S. Bernet, and M. Ritsch-Marte, *Appl. Phys. Lett.* **84**, 816 (2004).
7. C. Heinrich, S. Bernet, and M. Ritsch-Marte, *New J. Phys.* **8**, 36 (2006).